

CFD simulation of biomass grate furnaces with a comprehensive 3D packed bed model

Ramin Mehrabian^{1,2,*}, Stefan Stangl¹, Robert Scharler^{1,2,3}, Ingwald Obernberger^{1,2,3}, Alexander Weissinger⁴

¹BIOENERGY 2020+ GmbH, Inffeldgasse 21b, 8010 Graz, Austria

²Institute for Process and Particle Engineering, Graz University of Technology, Inffeldgasse 21b, A-8010 Graz, Austria

³BIOS BIOENERGIESYSTEME GmbH, Inffeldgasse 21b, A-8010 Graz, Austria

⁴KWB - KRAFT UND WÄRME AUS BIOMASSE GmbH, Industriestrasse 235, A-8321 St. Margarethen/Raab, Austria

Abstract

A 3D CFD model for biomass packed bed combustion has been developed at BIOENERGY 2020+ in co-operation with BIOS BIOENERGIESYSTEME and KWB in a previous work [1]. It consists of an Euler-Granular model for hydrodynamics of gas-particle multiphase flow and a thermally thin particle model for combustion of biomass particles. In this paper, this model has been improved by the implementation of a layer model for thermally thick particles. The new packed bed model provides the advantages of considering the intra-particle species and temperature gradients and, accordingly, allows for parallel progress of the thermal conversion sub-processes. Moreover, the layer model considers a more realistic shape for biomass particles, e.g. cylinders. Enhanced models for pyrolysis and char oxidation are applied and char gasification reactions are included. Additionally, the products of char oxidation are CO and CO₂, whereas the ratio between these species changes depending on the particle temperature. The simulation of a small-scale underfeed stoker furnace has been successfully performed by the application of the new packed bed combustion model. The positions of the drying, pyrolysis and char burnout zones in the fuel bed as well as the temperature distribution among the particles seem to be plausible and could be confirmed by observations. Furthermore, a good qualitative agreement concerning the flue gas temperatures measured by thermocouples at different positions in the combustion chamber and CO emissions measured at boiler outlet could be achieved.

1. Introduction and objectives

CFD simulation techniques are an efficient tool for the design and optimisation of biomass grate furnaces. They have successfully been applied to predict the turbulent reactive flow in combustion chambers of furnaces [2-5]. However, at present there is a lack of reasonably accurate and computationally efficient simulation tools for packed bed biomass combustion, which directly integrate the packed bed modelling into the available models for the turbulent reactive flow.

A combination of several sub-processes such as heat-up, drying, pyrolysis and char burnout represents the thermal conversion of solid biomass particles. Depending on the size and the physical properties of the biomass particles, temperature and species gradients may develop inside the particles causing intra-particle transport processes. The group of particles with gradients inside the particle and simultaneous progress of the different conversion stages is called thermally thick particles. The biomass particles in grate furnaces typically belong to this group. Several studies have been performed to describe the thermal conversion of a single thermally thick biomass particle [6-11].

In this work the packed bed is considered as an ensemble of representative particles, where each of these particles undergoes thermal conversion processes. The conversion of these particles is modelled by a thermally thick particle model. The layer model is able to describe the most essential characteristics of the thermal conversion of the thermally thick biomass particles, such as the intra-

* Corresponding author: Tel: +43 316 873 9232; email: ramin.mehrabian@bioenergy2020.eu

particle temperature gradient, the overall mass loss, the particle shrinkage and the change of physical properties during conversion. The layer model is applicable for cylindrical as well as spherical shapes. The particle model is implemented into ANSYS FLUENT as a User Defined Function (UDF) to perform the simulations of the entire biomass grate furnace. The hydrodynamics of the packed bed granular flow are modelled by the Euler-Granular model of ANSYS FLUENT. This model is based on the kinetic theory of granular flows and allows the consideration of inter-particle interactions which are of key importance when modelling packed beds.

Therefore, a new 3D packed bed model based on a combination of the Euler-Granular model for tracing the particle trajectories and the layer model for the thermal conversion of the thermally thick particles is presented. Then the model is applied to simulate the packed bed combustion in an underfeed stoker furnace.

2. Methodology

Packed bed modelling is divided into two parts, the hydrodynamics of the packed bed multiphase flow, and the thermal conversion of the biomass particles. The Euler-Granular model of ANSYS FLUENT is selected to simulate the packed bed multiphase flow. However, the Euler-Granular model does not enable the implementation of the layer model for the simulation of the thermal conversion of the particles via UDF. On the other hand, the Discrete Phase Model (DPM) of ANSYS FLUENT is not suitable for particle tracking under packed bed conditions, because it ignores the particle-particle collisions. However, its multi-component particle model provides a possibility to hook the layer model to ANSYS FLUENT. Therefore, a simulation with non-reacting flow based on the Euler-Granular model was performed and the simulated velocity field of the granular phase was stored as a User Defined Memory (UDM). Then, these data were used to prescribe the particle velocities in the DPM simulations by means of a UDF. Since the Euler-Granular simulation is without reactions, the effect of particle shrinkage on their movements is not considered.

As mentioned, the layer model considers the intra-particle species and temperature gradients and, accordingly, allows to consider the parallel progress of the thermal conversion sub-processes. Moreover, the layer model provides the advantages of considering a more realistic shape for biomass particles, e.g. finite cylinders, in contrast to the former packed bed model, where particles were approximated as spherical. Drying occurs at a fixed boiling temperature and its progress is limited by the transport of heat inside the particle. Pyrolysis is modelled by three independent competitive reactions for cellulose, hemicellulose, and lignin. The char oxidation and gasification reactions are assumed to be limited by the kinetic rate as well as the mass transport rate, which is calculated based on Sherwood correlations for cylindrical particles. The products of char oxidation are CO and CO₂, whereas the ratio between these species changes depending on the particle temperature. In the next sub-sections, both parts of the packed bed model are explained.

The turbulent reactive flow in the combustion chamber above the packed bed is described by the following models: the Realizable $k-\epsilon$ model for turbulence; the Eddy Dissipation Model with modified Magnussen constants [2] for turbulence-chemistry interaction, a global 4-step mechanism considering volatiles, CH₄, CO, CO₂, H₂, H₂O, and O₂ for gas phase combustion [2-3], and the Discrete Ordinates Model for radiation.

2.1. Hydrodynamics of the packed bed

In the Euler-Granular model all the particles are assumed to be identical, specified by their mean diameter (spherical shape) and density. Therefore handling a poly-disperse system, i.e. a system with different particle sizes, requires several solid phases corresponding to the number of particle diameter classes. In this approach the gas-solid multiphase flow is considered as interpenetrating continua. It incorporates the concept of the volume fraction. The volume fraction represents the space occupied by

each phase and they are assumed to be continuous functions of space and time and their sum is equal to one. The conservation equations for solid and gas phase have a similar structure because of the same Eulerian treatment. The solid phase momentum equation is similar to that of the gas phase with some additional terms, i. e. solid pressure (p_s), solid stress-strain tensor ($\bar{\tau}_s$) and inter-phase momentum exchange coefficient (K_{gs}), accounting for the solid phase behaviour:

$$\frac{\partial}{\partial t}(\alpha_s \rho_s \bar{u}_s) + \nabla \cdot (\alpha_s \rho_s \bar{u}_s \bar{u}_s) = -\alpha_s \nabla p - \nabla p_s + \nabla \cdot \bar{\tau}_s + \alpha_s \rho_s \bar{g} + (K_{gs}(\bar{u}_g - \bar{u}_s) + \dot{m}_{gs} \bar{u}_g - \dot{m}_{sg} \bar{u}_s) \quad (1)$$

where ρ_s is the density of the solid phase [$kg.m^{-3}$], \bar{u} is the velocity vector [$m.s^{-1}$] and α_s is the volume fraction of the solid phase [-]. \dot{m}_{gs} and \dot{m}_{sg} characterise the mass transfer [$kg.s^{-1}.m^{-3}$] from the gas to the solid phase and contrariwise, respectively.

There are several correlations for these additional terms [12-17]. They have been driven by making an analogy between the particle-particle collisions and the kinetic theory of gases [18]. The concept of granular temperature is defined to represent the kinetic energy of random particle fluctuations around their mean velocities. A conservation energy equation is formulated for this kinetic fluctuation energy in which the kinetic energy is produced by shear stress and turbulence and dissipated by inelastic collisions and interaction with the fluid. The collisions between the particles are assumed to be a function of this kinetic fluctuation energy. A detailed description of the Euler-Granular model is presented in [1].

2.2. Thermal conversion of particles (layer model)

As mentioned, the second part of the packed bed model is the thermal conversion of the particles. It is performed by an in-house code (layer model). The layer model accounts for intra-particle transport processes and the simultaneous progress of the thermal conversion sub-processes.

To reduce the model complexities and calculation time, only the radial temperature gradient in the particle is considered. This is a usual simplifying assumption. Its validity was already addressed by Ha and Choi [19]. To apply the one-dimensional model for a finite cylindrical geometry, Thunman's discretisation approach [9] has been applied. This approach assumes that the particle boundary conditions are homogeneous and every point in the particle at a certain distance from the particle surface has the same temperature and conversion state. The particle is divided into four layers: drying layer, pyrolysis layer, char and ash layer. The boundaries between the layers are related to the conversion sub-processes: drying, pyrolysis and char burnout fronts. At the beginning of the thermal conversion process only drying is of relevance. Due to heating up, moisture starts to get released from the particle. The pyrolysis layer consists of dry biomass and is located around the drying layer as the drying front moves towards the particle centre. When pyrolysis commences, the dry biomass converts to char and volatiles. The volatiles leave the particle and the char builds a layer around the pyrolysis layer. Finally, char burnout also creates another layer which contains only ash and surrounds the char layer. As the conversion of the fuel particle proceeds, drying, pyrolysis and char burnout fronts move from the surface to the centre of the particle. Figure 1 shows the scheme of the layer model for a cylindrical particle at a certain time when all the sub-processes of thermal conversion are occurring.

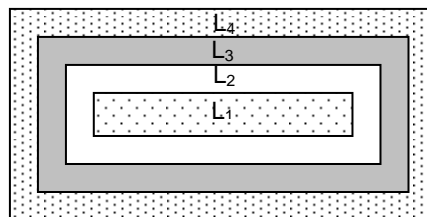


Figure 1: Scheme of the layer model; L₁...drying layer; L₂...pyrolysis layer; L₃...char layer; L₄...ash layer.

The conversion of each layer is simulated by separate sub-models. It is assumed that drying occurs at a fixed boiling temperature in an infinitely thin zone that separates the wet and the dry part of the particle. Such a steep drying front for the fast drying of biomass is reported almost by all drying models [20]. The drying process acts as a heat sink. It means that any amount of heat flow above the boiling temperature is consumed by the drying process. This approach to calculate the evaporation rate is the most often used model in literature, for instance [7, 10]. It is assumed that there is no resistance to mass transfer, and therefore the water vapour instantaneously leaves the particle. However, the cooling effect of the water vapour transfer through the particle is considered. Therefore the drying rate is controlled by the heat transfer.

Biomass pyrolysis is described by the decomposition of its three pseudo-components hemicellulose, cellulose, and lignin. This model implicitly assumes the hypothesis of an independent decomposition of these three constituents. An Arrhenius equation is used to describe the pyrolysis of each pseudo-component. The overall mass loss rate of a particle during pyrolysis is given as:

$$-\frac{dm}{dt} = \sum_{i=1}^3 c_i \frac{da_i}{dt} \quad (2)$$

where i is related to each pseudo-component, $c_i = m_{0,i} - m_{f,i}$ is a measure of the contribution of the partial decomposition processes to the overall mass loss $m_0 - m_f$. The conversion of each pseudo-component a_i can be expressed by:

$$a_i = \frac{m_{0,i} - m_i}{m_{0,i} - m_{f,i}} \quad (3)$$

where $m_{0,i}$ and $m_{f,i}$ are the initial and the final mass [kg] of the i^{th} pseudo-component, respectively. m_i is the actual mass [kg] of the i^{th} pseudo-component.

The pseudo-components are all assumed to decompose individually according to a first-order reaction, therefore the conversion rate of each pseudo-component is given by:

$$\frac{da_i}{dt} = A_i \exp\left(-\frac{E_i}{RT}\right)(1 - a_i) \quad (4)$$

where A is the pre-exponential factor [s^{-1}], E is the activation energy [$kJ.mol^{-1}$] and R is the universal gas constant [$kJ.mol^{-1}.K^{-1}$]. The empirical constants needed in the pyrolysis model are obtained from the fast heating rate experiments reported by Branca et al. [21].

The volatiles yielded from pyrolysis include a complex mixture and several hydrocarbons have been found in it. This complex mixture mainly consists of CO, CO₂, H₂O, H₂, light hydrocarbons and heavy hydrocarbons (tar). To simplify the combustion behaviour of the volatiles, the light and heavy hydrocarbons are lumped together and the chemical and physical properties of methane are assigned to this lumped hydrocarbon.

Char conversion models are more complicated than biomass pyrolysis models, as they are based on heterogeneous reactions for which both intrinsic kinetic and transport phenomena are important. It has been experimentally verified that char combustion is such a rapid reaction that it occurs in a very thin layer [22]. Due to the structure of the layer model, the char conversion reactions are assumed to occur at the interface between the char and the ash layer. Char oxidation with O₂ and gasification with CO₂, H₂O and H₂ are considered as char conversion reactions. There is clear evidence that both CO and CO₂ are primary products of char oxidation [23]. The ratio of CO to CO₂ production changes with temperature [24]. The heterogeneous reaction rate constants as well as the CO/CO₂ product ratio are listed in Table 1. The rate of char conversion reactions is a function of both kinetic rate at the reaction surface and mass transfer rate to/from the reaction surface. Assuming a global reaction rate of first order with respect to the oxidising/gasifying agent concentration leads to char conversion rate as:

$$\frac{dm_{ch}}{dt} = - \sum_{i=1}^4 \frac{\Omega_i M_c}{\frac{1}{k_i S} + \frac{1}{h_m S} + \frac{1}{\int_{\delta_{ash}} \frac{dr}{D_e S(r)}}} X_{\infty, i} \quad (5)$$

where $i = 1$ to 4 corresponds to the heterogeneous reactions in Table 1 and Ω is the stoichiometric ratio of moles of carbon per mole of oxidising/gasifying agent in the corresponding reaction. M_c , S , k_i , δ_{ash} and $X_{\infty, i}$ are the carbon molecular weight [$kg.kmol^{-1}$], the surface area of the char burnout front [m^2], the kinetic rate constant of heterogeneous reaction i [$m.s^{-1}$], the thickness of the ash layer [m] and the molar concentration of oxidising/gasifying agent of reaction i at the bulk flow [$kmol.m^{-3}$], respectively.

The mass transfer coefficient of reactant species in the boundary layer around the particle h_m [$m.s^{-1}$], is obtained by the Sherwood number. The effective diffusivity of the ash layer D_e [$m^2.s^{-1}$], depends on the ash porosity ϕ [-], the tortuosity η [-], and the molecular diffusivity of the penetrating gaseous component D_a [$m^2.s^{-1}$]:

$$D_e = \frac{\phi}{\eta} D_a \quad (6)$$

The tortuosity can be replaced by the inverse of the porosity [26, 27]:

$$D_e = \phi^2 D_a \quad (7)$$

Table 1: Heterogeneous reaction rate constants [25]

$\Omega C + O_2 \rightarrow 2(\Omega - 1)CO + (2 - \Omega)CO_2$	$k = 1.715T \exp(-9000/T)$ $\Omega = \frac{2[1 + 4.3 \exp(-3390/T)]}{2 + 4.3 \exp(-3390/T)}$
$C + CO_2 \rightarrow 2CO$	$k = 3.42T \exp(-15600/T)$
$C + H_2O \rightarrow CO + H_2$	$k = 3.42T \exp(-15600/T)$
$C + 2H_2 \rightarrow CH_4$	$k = 3.42 \times 10^{-3} T \exp(-15600/T)$

Since particle shrinkage during drying is much lower compared to that occurring during pyrolysis and charcoal combustion [28], it is postulated that during drying, the size of the particle remains constant and its density decreases. However, during the pyrolysis and char burnout, due to the particle mass loss and consideration of different densities for dry wood, char and ash, both shrinkage and density change are considered in the layer model.

The external surface of the particle exchanges heat and mass with the surroundings. Boundary conditions are required to complete the system of equations. The symmetry boundary condition is applied for the energy equation at the particle centre which leads to zero heat flux. The specified gradient boundary condition is used at the particle surface:

$$\lambda \frac{dT}{dr} \Big|_{r=\frac{d}{2}} = \varepsilon \sigma (T_{rad}^4 - T_{r=\frac{d}{2}}^4) + h_{conv} (T_{conv} - T_{r=\frac{d}{2}}) \quad (8)$$

where d is the actual diameter of the particle [m]. λ , ε and σ are the thermal conductivity [$W.m^{-1}.K^{-1}$], emissivity (0.85) [-] and Stefan-Boltzmann constant [$W.m^{-2}.K^{-4}$], respectively. h_{conv} is the convective heat transfer coefficient [$W.m^{-2}.K^{-1}$]. It is determined by an appropriate correlation for the Nusselt number. For spherical particles the Ranz-Marshall correlation and for cylindrical particles the correlation proposed by Churchill and Bernstein are applied [29].

3. Investigated grate system and fuel applied

The grate of the KWB underfeed stoker furnace is shown in Figure 2. The fuel, softwood spruce pellets, is fed on the grate from below and is transported towards the outer edge of the grate. Primary air is supplied through the grate from nozzles at the bottom which form a concentric ring with the fuel feeding tube in the centre. In the simulation the primary air nozzles are represented by three concentric rings as it is shown in Figure 2.

Since wood pellets are a very homogeneous biomass fuel, it is realistic to assume an average biomass size and average physical properties to characterise them. Therefore, based on the average size of the pellets, a length and a diameter are used in the calculations of the layer model. Moreover, in the Euler-Granular model the solid phase was represented only by one particle size class, i.e. one solid phase. It considerably reduces the calculation time. Hjertager reported a quadratical increase of computational effort with the number of phases [30]. However, the particles in the Euler-Granular model can only be represented as spherical particles. Thus the average diameter of the pellets is calculated based on the equivalent volume. The fuel analysis and operating conditions and other input parameters used in the simulations of the KWB underfeed stoker grate furnace are listed in Table 2.

Since the plant technology investigated is restricted know how of the company KWB-Kraft und Wärme aus Biomasse GmbH, only selected results, relevant concerning the 3D packed bed combustion model development, are presented in the next part.

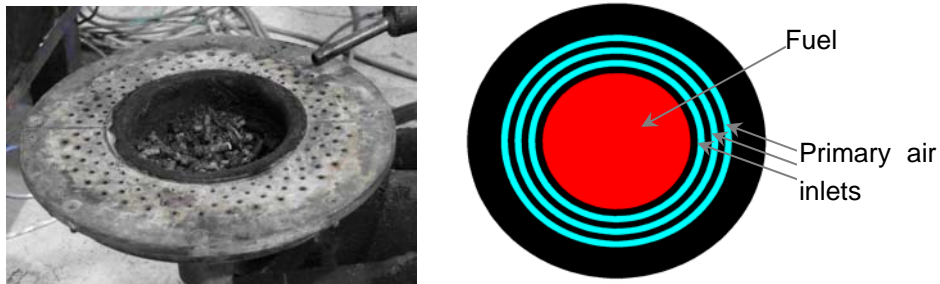


Figure 2: Left: grate of the KWB underfeed stoker furnace; right: scheme of the grate used for simulations

Table 2: Parameters used in the simulations

Ultimate Analysis [wt% d.b.]		Proximate Analysis [wt% d.b.]	
C	50.1	Moisture content [w.b.]	8.12
H	5.7	Volatiles	77.1
O	43.72	Fixed carbon	22.54
N	0.12	Ash	0.36
Total air ratio	1.58	Average diameter [m]	0.006
Primary air ratio	0.64	Average length [m]	0.018
Nominal power [kW]	20.0	Fuel feed rate [kg/h]	5.023
	ρ [kg.m ⁻³]	c_p [J.kg ⁻¹ .K ⁻¹]	λ [W.m ⁻¹ .K ⁻¹]
Dry wood	1120	1500+T	0.14+6.5e ⁻⁴ T
Char	200	420+2.09T+6.85e ⁻⁴ T ²	0.071
Ash	300	420+2.09T+6.85e ⁻⁴ T ²	1.2
Water	998.2	4182	0.6
	Hemicellulose	Cellulose	Lignin
A [s ⁻¹]	2.527e11	1.379e14	2.202e12
E [kJ.mol ⁻¹]	147	193	181
C [-]	0.26	0.64	0.10
	Magnussen empirical constants		
A [-]	0.8	B [-]	0.5

4. Results and discussion

Figure 3 shows the contours of the release rates of H₂O, volatiles, CO and CO₂ along a vertical cross section through the grate axis. CO and CO₂ are the products of char oxidation. Here, the positions of the drying, pyrolysis, and char burnout zones inside the fuel bed are illustrated. In addition, the particle tracks on the grate coloured by the release rates of these species are presented in Figure 4. As it is shown in these figures, the three sub-processes of particle thermal conversion sequentially happen with an overlap between each other, particularly between pyrolysis and char burnout. Drying takes place in the centre of the bed above the fuel inlet. As it is shown in Figure 4, drying ends before the pellets reach the fuel bed surface. Afterwards, particles start to release volatiles along their radial path to the outer edge of the grate. The remaining char mainly reacts with oxygen above the outer primary air injection region.

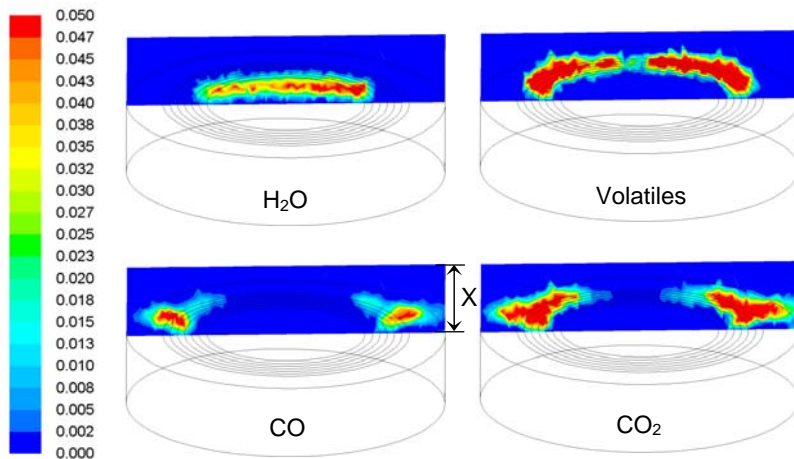


Figure 3: Contours of release rates of different species during the thermal conversion of the pellets [mg/s] at a vertical cross section through the grate axis; $x= 5\text{cm}$

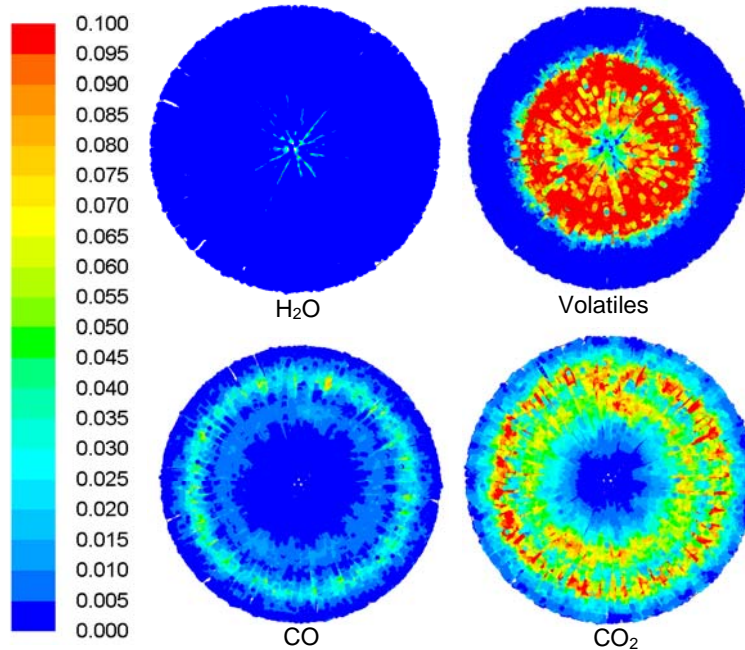


Figure 4: Particle tracks on the grate coloured by release rates of different species [mg/s]

According to the simulation results, less than 1.2 wt.% of the fixed carbon is consumed by the gasification reactions. It is due to their much slower reaction rates in comparison with the rate of the oxidation reaction. Using the CO/CO₂ product ratio in dependence of particle temperature, as in Table 1, results in an average value of about 0.48 for this ratio. It means the char oxidation produces more CO₂ than CO. It is attributed to the fact that at high temperatures most of the produced CO rapidly oxidises to CO₂ in the pores of the particles as well as in a layer so close to the particle surface that it gives its heat of combustion to the particle [31, 32]. Therefore, it is plausible to assume this produced CO₂ as the product of the heterogeneous char oxidation reaction.

The flue gas temperatures along a vertical cross section of the combustion chamber as well as the particle tracks coloured by the simulated particle temperatures are shown in Figure 5. Additionally, a picture taken from a window at the top of the furnace is enclosed in Figure 5 for comparison. However, from this picture the entire bed can not be seen, due to a reduction of diameter at the position where the secondary air is injected. The dashed line in Figure 5-b approximately represents the part of the bed which can be seen from the window at the top.

The predicted locations of the fuel conversion stages in the fuel bed are an explanation of the simulated particle temperatures in Figure 5. It can be seen that at the surface of the fuel bed, the lowest particle temperatures occur in the centre, which is due to the fact that drying takes place there. Afterwards, the particle temperatures increase due to the external heat flux and the volatile components of the particles are released. Char oxidation further increases the particle temperatures. The highest particle temperatures at the surface of the fuel bed occur at the outer primary air inlet region, due to the higher rate of char oxidation and the comparatively small size of the particles. Afterwards, the temperatures of the ash particles sharply decrease at the outer edge of the grate. The maximum predicted particle temperatures in the bed (1400 K) show an improvement in comparison with former simulations (1100 K) [1], because the new results are in good agreement with previous experiments performed in a lab-scale batch reactor [33]. It implies that both carbon monoxide and carbon dioxide have to be considered as the products of the char oxidation reaction. The results regarding to the variations of the particle temperatures are in good agreement with the picture taken from the top of the furnace.

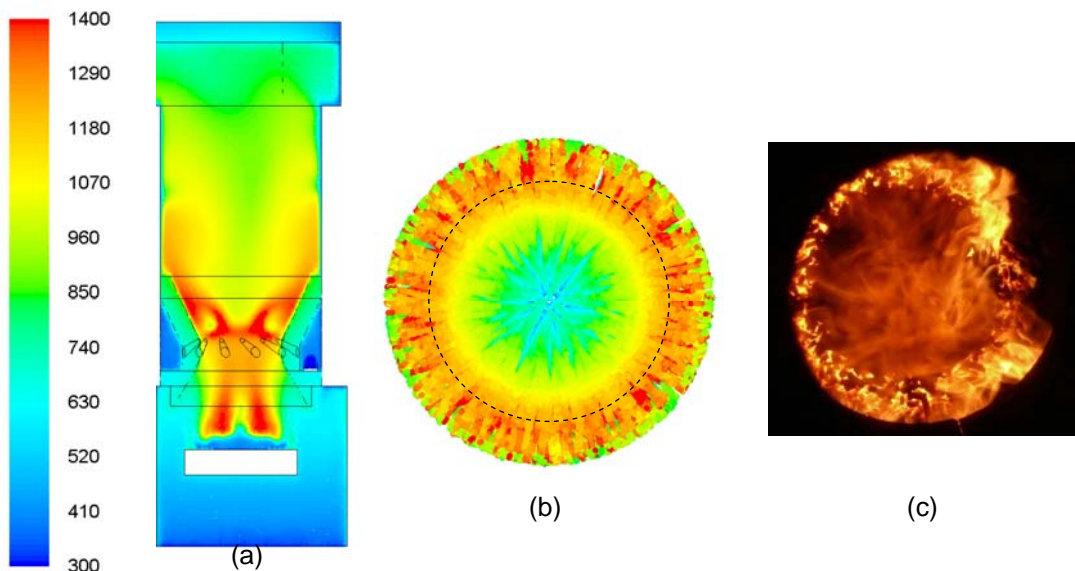


Figure 5: a) Contours of flue gas temperatures (K) along a vertical cross section of the combustion chamber; b) Particle tracks on the grate coloured by particle temperatures (K); c) Visual observation from a window at the top of the furnace.

5. Conclusion

The previous 3D CFD based packed bed combustion model [1] has been improved. In the new model, in contrast to the former one, the biomass particles are considered as thermally thick, i.e. the intra-particle species and temperature gradients are considered. Therefore, the parallel progress of the thermal conversion sub-processes is accounted for. Moreover, the layer model considers the particles as cylinders. The char burnout and pyrolysis models are more comprehensive than in the former model. The char gasification reactions are included. The products of char oxidation are CO and CO₂, whereas the ratio between these species changes depending on the particle temperature.

The model has been successfully applied to simulate a 20 kW KWB underfeed stoker grate furnace. The maximum predicted particle temperatures in the bed are in agreement with values from experiments at a lab-scale batch reactor. Hence, the new 3D packed bed model can better predicate the particle temperatures and also burnout conditions. This is of great advantage for a correct description of particle burnout and the release of gaseous and ash forming species. The char burnout model predicts the unburned char to be less than 1 wt.%, which is in good agreement with experiences concerning the burnout quality of the grate ash. Moreover, the results regarding variations of the particle temperatures at the bed surface and the locations of the fuel conversion stages are in qualitative agreement with visual observations of the packed bed. Hence, the new 3D packed bed model provides the following advantages for the simulation of grate furnaces:

- The effect of particle related parameters, e.g. size, physical properties and moisture content, as well as operating conditions, e.g. air distribution below the grate and air staging conditions in a furnace, on the thermal conversion of the entire packed bed can be investigated.
- Modelling the hydrodynamics of the packed bed by the granular kinetic theory allows to approximate the particle movements on the grate under consideration of particle-particle collisions.
- Due to consideration of the particles as thermally thick, the particle temperatures and consequently the mass loss rate during the thermal conversion of the particles can be better predicted. Hence, the predicted release profiles of species and energy from the fuel bed are closer to reality.

As next steps of model improvement, the development of an enhanced heat transfer model inside the packed bed and the application of an appropriate gas-solid multiphase model to avoid the separate simulation for the dynamics of the particle movement in the bed are foreseen.

6. References

- [1] Mehrabian R., Scharler R., Weissinger A., Obernberger I., 2010: Optimisation of biomass grate furnaces with a new 3D packed bed combustion model - on example of a small-scale underfeed stoker furnace. Proceedings of the 18th European Biomass Conference, Lyon, France, pp. 1175-1183.
- [2] Scharler R., Fleckl, T., Obernberger, I., 2003: Modification of a Magnussen Constant of the Eddy Dissipation Model for biomass grate furnaces by means of hot gas in-situ FT-IR absorption spectroscopy. Progress in Computational Fluid dynamics, Vol. 3, pp. 102-111.
- [3] Scharler R., Obernberger I., 2000: Numerical optimisations of biomass grate furnaces. Proceedings of the 5th European Conference on Industrial Furnaces and Boilers INFUB, Portugal.
- [4] Scharler R., Zahirovic S., Schulze K., Kleditzsch S. Obernberger I., 2006: Simulationsgestützte Auslegung und Optimierung von Biomassefeuerungs- und Kesselanlagen – Einsatzmöglichkeiten, Stand der Technik und innovative Methoden. Österreichische Ingenieur- und Architektenzeitung, Vol. 10-12, pp. 296-309.
- [5] Scharler, R., 2001: Entwicklung und Optimierung von Biomasse-Rostfeuerungen durch CFD-Analyse. Ph.D. thesis, Graz University of Technology, Austria.
- [6] Peters B., 2002: Measurements and application of a discrete particle model (DPM) to simulate combustion of a packed bed of individual fuel particles. Combustion and Flame, Vol.131, pp. 132-146.
- [7] Bruch C., Peters B., Nussbaumer T., 2003: Modelling wood combustion under fixed bed conditions. Fuel, Vol. 82, pp. 729-738.
- [8] Wurzenberger J.C., Wallner S., Raupenstrauch H., Khinast J.G., 2002: Thermal conversion of biomass: Comprehensive reactor and particle modeling. AIChE J , Vol. 48, pp. 2398-2410.

- [9] Thunman H., Leckner B., Niklasson F., Johnsson F., 2002: Combustion of wood particles - a particle model for eulerian calculations. *Combustion and Flame*, Vol. 129 pp. 30-46.
- [10] Porteiro J., Granada E., Collazo J., Patino D., Moran J.C., 2007: A Model for the combustion of large particles of densified wood. *Energy & Fuels*, Vol. 21, pp. 3151-3159.
- [11] Lu H., Robert W., Peirce G., Ripa B., Baxter L.L., 2008: Comprehensive Study of Biomass Particle Combustion. *Energy & Fuels*, Vol. 22, pp. 2826-2839.
- [12] Gidaspow D., Bezburuah R., Ding J., 1992: Hydrodynamics of Circulating Fluidized Beds, Kinetic Theory Approach. In O. E. Potter and D. J. Nicklin, Eds., *Fluidization VII*, Engineering Foundation, pp. 75-82.
- [13] Lun C. K. K., Savage S. B., Jeffrey D. J., Chepurnyi N., 1984: Kinetic theories for granular flow: inelastic particles in Couette flow and slightly inelastic particles in a general flow field. *J. Fluid Mech.*, Vol. 140, pp. 223-256.
- [14] Gidaspow D., 1994: *Multiphase flow and fluidization*. Academic Press, Boston.
- [15] Syamlal M., Rogers W., O'Brien T. J., 1993: *MFIX Documentation: Volume 1, Theory Guide*. National Technical Information Service, Springfield, VA, DOE/METC-9411004, NTIS/DE9400087.
- [16] Gidaspow D., Jayaswal U. K., Ding J., 1991: Navir-Stokes Equation Model for Liquid-Solid Flows Using Kinetic Theory. *Liquid Solid Flows*, Vol. 118, New York: ASME, pp. 165-178.
- [17] Sinclair J. L., Jackson R., 1989: Gas-particle flow in a vertical pipe with particle-particle interactions. *AIChE Journal*, Vol. 35, pp. 1473-1486.
- [18] Chapman S., Cowling T.G., 1970: *The mathematical theory of non-uniform gases*. Cambridge University Press, Cambridge.
- [19] Ha M.Y., Choi B.R., 1994: A numerical study on the combustion of a single carbon particle entrained in a steady flow. *Combustion and Flame*, Vol. 97, pp. 1-16.
- [20] Di Blasi C., 1998: Multi-phase moisture transfer in the high-temperature drying of wood particles. *Chemical Engineering Science*, Vol. 53, pp. 353-366.
- [21] Branca C., Albano A., Di Blasi C., 2005: Critical evaluation of wood devolatilization mechanisms. *Thermochim Acta*, Vol. 429, pp. 133-141.
- [22] Gomez-Barea A., Leckner B., 2010: Modelling of biomass gasification in fluidized bed. *Prog. Energy Combustion Science*, Vol. 36, pp. 444-509.
- [23] Tognotti L., Longwell J.P., Sarofim A.F., 1990: The products of the high temperature oxidation of a single char particle in an electrodynamic balance. *Proc. Combustion Inst.*, Vol. 23, pp. 1207-1213.
- [24] Evans D.D., Emmons H.W., 1977: Combustion of wood charcoal. *Fire Saf J*, Vol1, pp. 57-66.
- [25] Johansson R., Thunman H., Leckner B., 2007: Influence of intraparticle gradients in modeling of fixed bed combustion. *Combustion and Flame*, Vol. 149, pp. 49-62.
- [26] Froment G.F., Bischoff K.B., 1990: *Chemical reactor analysis and design*. New York: John Wiley & Sons.
- [27] Patisson F., Francois M.G., Ablitzer D., 1998: A non-isothermal, non-equimolar transient kinetic model for gas-solid reactions. *Chem. Eng. Sci.*, Vol. 53, pp. 97-708.
- [28] Kumar R.R., Kolar A.K., Leckner B., 2006: Shrinkage characteristics of Casuarina wood during devolatilization in a fluidized bed combustor. *Biomass Bioenergy*, Vol. 30, pp. 153-165.
- [29] Incropera F.P., De Witt D.P., 1990: *Introduction to heat transfer*. 2nd ed. New York: John Wiley & Sons.
- [30] Hjertager B. H., Solberg T., Ibsen C. H., Hansen K. G., 2003: Multi-Fluid CFD modelling of fluidised bed reactors. Invited Presentation Computational Fluid Dynamics in Chemical Engineering III, Davos, Switzerland.
- [31] Hayhurst A.N., Parmar M.S., 1998: Does solid carbon burn in oxygen to give the gaseous intermediate CO or produce CO₂ directly? Some experiments in a hot bed of sand fluidized by air. *Chem. Eng. Sci.*, Vol. 53, pp. 427-438.
- [32] Wang F.Y., Bhatia S.K., 2001: A generalised dynamic model for char particle gasification with structure evolution and peripheral fragmentation. *Chem. Eng. Sci.*, Vol. 56, pp. 3683-3697.
- [33] Dahl J., Obernberger I., 2004: Evaluation of the combustion characteristic of four perennial energy crops. Proceedings of the 2nd world conference and exhibition on biomass for energy, Rome, Italy.